

physica **p** status **s** solidi **S**

www.pss-journals.com

reprint



Effect of deposition temperature on transparent conductive properties of γ -CuI film prepared by vacuum thermal evaporation

Min Zi^{1,2}, Juan Li^{1,2}, Zichao Zhang^{1,2}, Xuesong Wang³, Jun Han^{1,2}, Xiaopeng Yang^{1,2}, Zhiwen Qiu^{1,2}, Haibo Gong^{1,2}, Ziwu Ji³, and Bingqiang Cao^{*1,2}

¹ Key Laboratory of Inorganic Functional Materials, University of Jinan, Jinan 250022, P.R. China

² School of Materials Science and Engineering, University of Jinan, Jinan 250022, P.R. China

³ School of Physics, Shandong University, Jinan 250100, P.R. China

Received 11 January 2015, revised 9 March 2015, accepted 9 March 2015

Published online 28 March 2015

Keywords conductivity, CuI, optical absorption, thermal evaporation, thin films

* Corresponding author: e-mail: mse_caobq@ujn.edu.cn, Phone/Fax: +86-531-8973-6292

Copper (I) iodide (CuI) films are grown on glass substrates with a direct vacuum thermal evaporation method, and the effect of substrate temperature on their photoluminescence and transparent conductive properties is discussed. The X-ray diffraction (XRD) measurement identifies the polycrystalline CuI film has γ -phase with (111) preferential growth direction. When the substrate temperature is optimised at

120 °C, the average transmittance is about 90% in the wavelength range of 410–1500 nm. The electrical properties measured by Hall effect show the lowest resistivity of $1.0 \times 10^{-2} \Omega\text{cm}$ with hole concentration of $3.0 \times 10^{19} \text{cm}^{-3}$ and mobility of $25 \text{cm}^2 \text{V}^{-1} \text{s}^{-1}$. These results indicate that direct thermal deposition is a simple method to grow high quality p-type CuI films.

© 2015 WILEY–VCH Verlag GmbH & Co. KGaA, Weinheim

1 Introduction Recently, much attention has been focused on copper (I) iodide (CuI) due to its large band gap (3.1 eV) and unique optical and electrical properties [1, 2], which makes it useful for promising applications in light emitting diodes (LED) and fully solid-state dye-sensitised solar cells as a hole conductor [3]. CuI is a halogenide semiconductor with three crystalline phases: γ -CuI (below 350 °C), β -CuI (between 350 and 392 °C) and α -CuI (above 392 °C) [4, 5]. The γ -phase with zinc-blende structure is one of the important I–VII p-type semiconductors.

CuI has been prepared with various methods. As early as 1908, Bädeker first intentionally grew doped CuI semiconductor by changing the iodine concentration [6]. Then Schein et al. prepared CuI films with the iodination of Cu films and the electrical parameters measured by Hall effect were hole concentration $p = 5 \times 10^{18} \text{cm}^{-3}$, hole mobility $\mu = 6 \text{cm}^2 \text{V}^{-1} \text{s}^{-1}$ and resistivity $\rho = 0.2 \Omega\text{cm}$ [7]. But, the optical transmittance in the visible spectral range was only 49% due to high roughness and light scattering. However, the

CuI films prepared with evaporation exhibit strong Fabry–Pérot interferences and an average transparency of about 80% in the visible spectral range [8]. Zhu et al. reported that CuI thin films grown with a pulse laser deposition (PLD) technique exhibiting the resistivity of 0.1–1 Ωcm and a transmittance of about 60–80% in the 410–1000 nm range [9]. Inudo et al. reported CuI films formed by spin coating and subsequent annealing with typical resistivity of 0.3–5 Ωcm and mobility of $0.5\text{--}2 \text{cm}^2 \text{V}^{-1} \text{s}^{-1}$ [10]. Compared with these reports, Tanaka et al. obtained CuI films by vacuum evaporation techniques with the same transmittance as RF-DC coupled magnetron sputtering, while the reported resistivity was $10^{-2} \Omega\text{cm}$ [11]. Considering the previous reports, the resistivity was too high to make it widely used in LED and the transmittance was also too low to be applied for fully solid-state dye-sensitised solar cells as a window layer. Consequently, it is necessary to prepare CuI films with high transmittance and low resistivity.

In this paper, we reported CuI films with both high transparency and conductivity. We used a simple thermal

vacuum evaporation technique to grow CuI films and studied the effect of substrate heating temperature on their physical properties. The morphology and structure of CuI films are investigated by SEM, X-ray diffraction (XRD) and X-ray photoelectron spectroscopy (XPS). The optical and electrical properties were investigated with the transmittance, photoluminescence spectrum and Hall effect measurements.

2 Experimental The CuI thin films were deposited on glass substrates in a vacuum thermal evaporation chamber. The pressed CuI powders (99.5% purity, Alfa) were placed in the evaporation boat. Corning glass (1737) sheets were cleaned in an ultrasonic bath with acetone for 10 min and rinsed in deionised water before being loaded into the evaporation chamber. The deposition rate was monitored by a quartz crystal oscillator and controlled by a heated electrical current. At a fixed deposition rate of 0.1 \AA s^{-1} , CuI films were grown at different substrate temperatures. The thickness of the CuI film was controlled by a film thickness monitor (FTM-V 106, Shanghai Taiyao Vacuum).

Morphology studies of CuI films were performed with a field emission scanning electron microscope (FE-SEM, Quanta 250, FEI). X-ray diffraction (XRD, D8-Advance, Bruker) was used to examine the crystal structure of the CuI films. The exact chemical states of the constituent elements were measured with X-ray photoelectron spectroscopy (XPS, ESCALAB 250, Thermo Fisher Scientific). The transmittance spectra were measured with a UV-vis-NIR spectrophotometer (UV-3600, Shimadzu) equipped with an integrating sphere. For temperature-dependent photoluminescence (PL) measurement, the sample was mounted in a closed-cycle He cryostat and the temperature was controlled from 5.5 to 300 K. The PL signal from the sample was dispersed by a Jobin-Yvon iHR320 monochromator and detected by a thermoelectrically cooled synapse CCD detector. The electrical properties were recorded with a Hall effect measurement system (ET-9000, Eastchanging) using van der Pauw geometry.

3 Results and discussion

3.1 Structural analysis of CuI films Figure 1(a–d) shows the SEM images of CuI films grown at various temperatures on glass substrates. The surface morphologies of CuI films show clear variations with increasing substrate temperature. The corresponding XRD patterns of the CuI films are shown in Fig. 1(e). It is observed that compared with the standard PDF card (JCPDS 06-0246), the phase of as-prepared CuI films for all substrate temperatures is γ -CuI. The main diffraction peaks are identified as (111) and (222), exhibiting preferential growth along the $\langle 111 \rangle$ direction. The (111)-face is a close-packed plane with the lowest energy [12]. As a general consideration of the stability energy, the growth rate along (111) is the fastest and (111) is the preferred orientation.

Most grains appear with triangular shape (type B) and a well-defined azimuthal orientation as shown in Fig. 1(b),

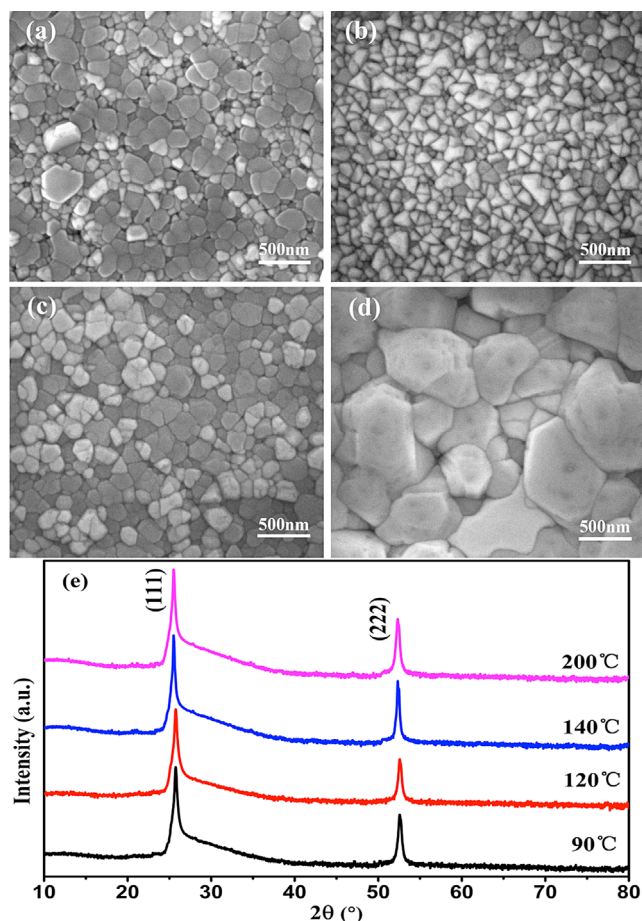


Figure 1 SEM images of CuI films deposited at different substrate temperature, (a) 90 °C, (b) 120 °C, (c) 140 °C, (d) 200 °C and (e) the corresponding XRD patterns (logarithmic intensity scale).

which is consistent with Kim's report [13]. However, we note that the CuI thin film exhibits more hexagonal shaped grains (type A) in other SEM images. As (111) is the dominating XRD peak, both must be (111) oriented. The formation of hexagonal shape grains in Fig. 1(a) can be understood with domain rotation of two triangular grains [8]. When the substrate temperature is 120 °C, the triangular grains in Fig. 1(b) are very ordered. The coalescence of neighbouring grains is observed when the relative orientation is the same. Therefore, we believe the growth in this case is near the thermodynamic equilibrium state. Type A and B both appear in Fig. 1(c), which is caused by the grains rearrangement when the substrate temperature further increases. The grain growth rate is too fast when the substrate is heated at 200 °C. Thus, the grains in Fig. 1(d) are much bigger than the others.

XPS analyses were carried out in order to investigate the exact chemical states of the constituent elements, as shown in Fig. 2. There is no other peak in the survey spectra compared with the reported XPS data of CuI [14] which can demonstrate that the films are of pure phase. The peaks

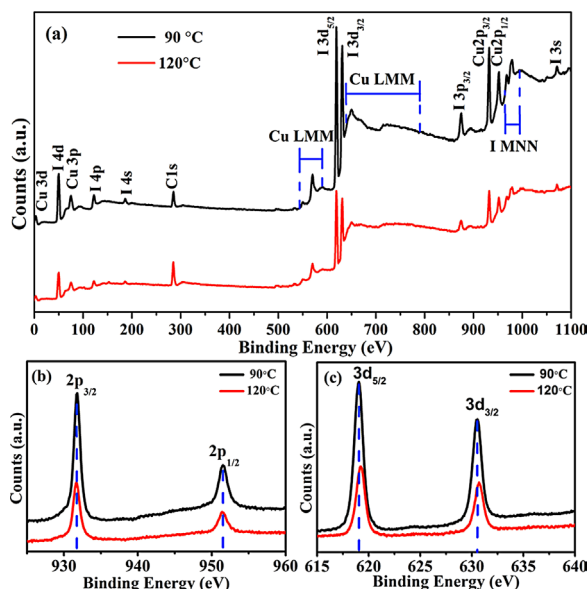


Figure 2 XPS spectra of survey spectra of CuI films (a), Cu 2p (b) and I 3d (c) core levels of the CuI films deposited at 90 °C (black line) and 120 °C (red line).

located at 951 and 932 eV are mainly consistent with Cu 2p_{1/2} and Cu 2p_{3/2}, respectively. The oxidation state of Cu is +1, which can be proved by the absence of any shake-up satellite peak. The core level spectra of I⁻ consist of two peaks at 630.5 and 619 eV, which correspond to I 3d_{3/2} and I 3d_{5/2}, respectively. All the peaks of both CuI films are not exactly at the same binding energy, and there is a little shift to higher binding energy when the peaks of I 3d were observed carefully. The higher binding energy shift appears in the spectrum of CuI grown at 90 °C, comparing with 120 °C, which can be attributed to the iodine vacancy. It is reported that the higher binding energy is always associated with an anion vacancy [15]. The number of iodine vacancies is too small to reduce the surrounding Cu⁺ ions, so the Cu 2p peaks remain almost unchanged. Hence, it is firmly established that the Cu ion is only monovalent because the Cu 2p spectra lacks any other peaks.

3.2 Optical properties of CuI films deposited at different substrate temperature

The transmittance spectra of CuI films deposited at different substrate temperatures are shown in Fig. 3. The transmittance spectra show interference patterns, which suggest the CuI film thickness and surface are both uniform. When the substrate temperature is 120 °C, the wave-like transmittance spectra of CuI films have maximal transmittance of near 100% and average transmittance of about 90% in the wavelength range of 410–1500 nm. The reason for this is that if the heated substrate can provide enough kinetic energy, CuI precursor atoms can move to the optimum positions to crystallise well. The transmittance spectra of other films are similar to 120 °C, but the transmittance of film grown at 200 °C is

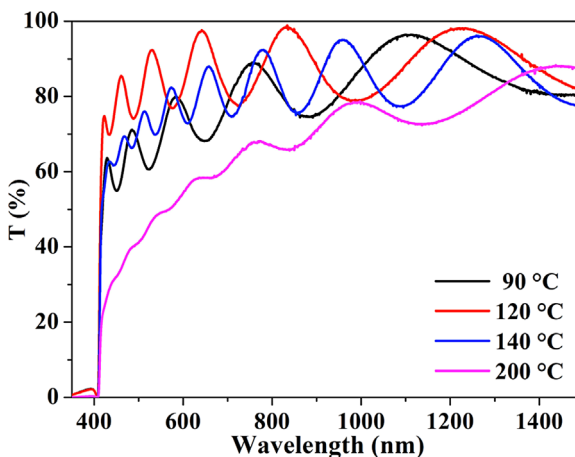


Figure 3 The transmittance spectra of the CuI films deposited at different substrate temperatures.

rather low. Possibly, this is caused by the different thermal expansion coefficients between glass substrate and CuI films. The CuI films adhere to glass substrate badly under high heating temperature that depresses the crystallisation and quality of the interface between the substrate and film. The absorption edges of all CuI films are located at almost same position (408 nm), which can be attributed to interband excitonic transition. The bandgap (E_g) of CuI films can be calculated from the relationship of $\alpha^2 \propto (h\nu - E_g)$, where α is the absorption coefficient and $h\nu$ is the photon energy. The α of the thin films is obtained for a given thickness (t) using $T = A \exp(-\alpha t)$, where A is a constant and $A \approx 1$ near the absorption edge [16]. Finally, the obtained E_g values of our CuI films deposited at different substrate temperatures are all about 3.04 eV. Many studies have reported the E_g of CuI is 3.1 eV [17], but several researchers have also reported an optical bandgap of CuI about 3 eV [18, 19], which is consistent with our results.

The PL spectra of CuI films deposited at various substrate temperatures were first measured under the excitation of a 313 nm Xe lamp at room temperature as shown in Fig. 4. The PL intensity was normalised with the strongest peak intensity for easy comparison. All the spectra have obvious PL peaks at around 410 nm near the absorption band edge. Another PL peak at about 420 nm was also observed. The emission peaks at 410 nm can be reasonably assigned to the free exciton (FX) or acceptor-bound exciton (A^0X) transition according to the energy position [20]. Whilst, the emission at 420 nm is reported to be ascribed to the presence of trap levels that probably are associated with iodine defects [21]. Although excess iodine has been associated with the presence of hole traps near the valence band maximum (VBM) of γ -CuI and the consequential emission at 420 nm, a recent first principles study shows that the introduction of iodide vacancies also gives new energy states slightly above the VBM of the stoichiometric crystal [22] and possibly accounts for the 420 nm emission

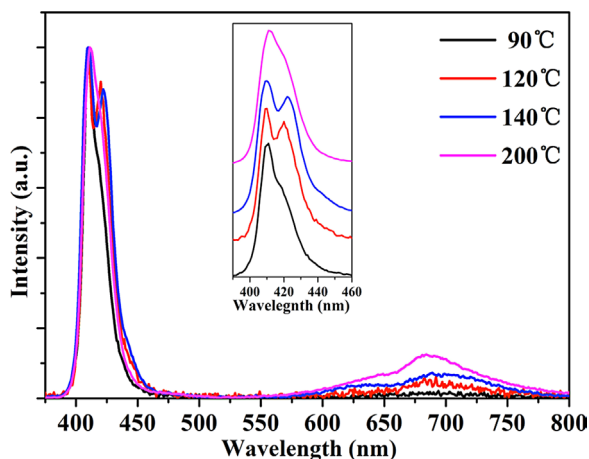


Figure 4 Room-temperature photoluminescence spectra of the CuI films grown at different substrate temperature from 90 to 200 °C as indicated. The inset shows details at 390–460 nm.

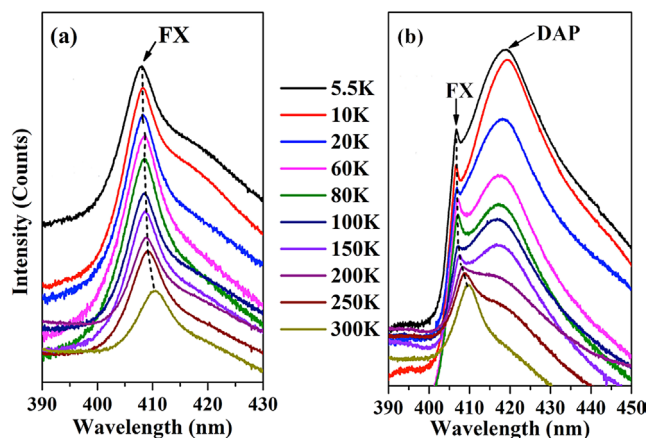


Figure 5 Temperature dependent PL spectra of the CuI films deposited at different temperatures, (a) 90 °C and (b) 120 °C (logarithmic intensity scale).

in our case. In addition, it has been consistently shown that photodecomposition of γ -CuI leads to an increase of the defect band at 420 nm [23]. Moreover, there is a much weaker emission peak near 680 nm in the red region, which is proved to be related to the iodine vacancy [24]. Its intensity increases with increasing substrate temperatures. When the PL measurement is excited with 313 nm light from a weak Xe lamp, the emission is sensitive to the sample surface. Iodine may be lost due to the high temperature when the CuI powder was heated in the evaporation boat as mentioned in the experiment procedure. High substrate temperature may also result in loss of iodine and its effect is more significant. Thus, the relatively stronger 680 nm peak appears at higher substrate temperatures.

To further study the PL properties of CuI, temperature-dependent PL spectra from 5.5 to 300 K of typical CuI films deposited at 90 and 120 °C were measured as shown in Fig. 5. In Fig. 5(a), these peaks at around 410 nm show a continuous redshift due to the bandgap shrinkage with temperature increase further proving their exciton origin. Their intensity decreases gradually due to the ionisation of part excitons from the acceptors and FX emission can still be observed at room temperature. But, due to peak broadening, no well-resolved emissions of free exciton and acceptor-related exciton can be observed at low temperature. Moreover, on the long wavelength side, a weak PL shoulder peak is observed, especially at low temperatures such as 5.5 K, which disappears quickly with increasing temperature. The possible origin is a donor–acceptor pair (DAP) emission [25] that can be observed more clearly for CuI film grown at 120 °C. In Fig. 5(b), besides these peaks around 410 nm with similar temperature-dependent behaviour, the DAP peak at about 420 nm becomes dominant at low temperature. The DAP peak intensity also decreases gradually with increasing temperature and finally becomes relatively weaker than the exciton peak above 200 K.

This temperature-dependent behaviour is typical for the thermal ionisation of shallow acceptors and donors via the pathway of $(D^0, A^0) \rightarrow D^+ + A^- + e + h$ [26]. The ionised free electrons and holes in the conduction and valence bands prefer to recombine in the form of excitons. As a result, the spectra are dominated by exciton emissions above 200 K.

3.3 Electrical properties of CuI films deposited at different substrate heating temperature

The electrical properties like resistivity (ρ), hole concentration (p) and mobility (μ) of CuI films were measured with Hall effect employing the van der Pauw method as shown in Fig. 6. The sign of the Hall constant was positive indicating the CuI films is of p-type conductivity. The resistivities of the CuI films were in the range of 10^{-2} – 10^{-1} Ω cm. The films obtained at the substrate temperature of 120 °C exhibited the lowest resistivities compared with other films and both the maximum hole mobility of 25 $\text{cm}^2 \text{V}^{-1} \text{s}^{-1}$ and carrier concentrations of

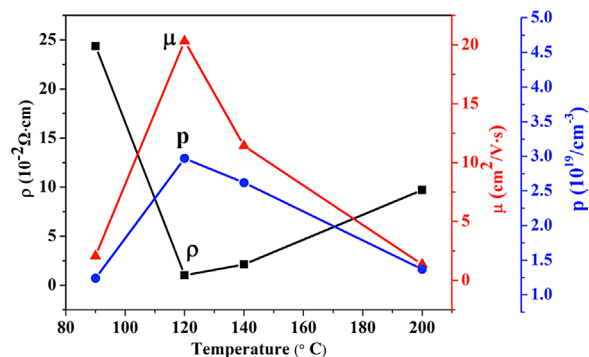


Figure 6 Resistivity (ρ , squares), hole concentration (p , circles) and mobility (μ , triangles) for CuI thin films grown at different substrate temperature.

$3.0 \times 10^{19} \text{ cm}^{-3}$ were achieved. The high mobility is near the value reported for bulk CuI single crystal grown with the hydrothermal method by Ding et al. [27].

The carrier concentration of CuI films first increase then decreases with increasing substrate temperature with a temperature inflexion of 120°C . It has been reported that the Cu vacancy (V_{Cu}) in CuI plays the role of the dominant native acceptor [28]. The evaporation of a trace amount of iodine from a CuI film that decreased the concentration of V_{Cu} , and the hole concentration decreased accordingly [10]. The hole mobility exhibits similar temperature-dependent behaviour to the carrier concentration. The crystallinity of CuI films at 120°C is better than the others as shown in Fig. 1. The main scattering mechanism leading to the observed decrease of mobility is grain boundary effects. The low resistivity at 120°C is attributed to the improvement of the grain boundaries, which leads to less carrier scattering and enhances the carrier mobility of CuI atoms. As a result of both carrier concentration and mobility obtaining the optimised values, the CuI film shows ten times smaller resistivity when the substrate temperature is 120°C .

4 Conclusions In summary, we investigated the substrate temperature effect on the CuI film physical properties grown on glass by vacuum thermal evaporation technique. The XRD measurement identified the CuI films were of polycrystalline γ -phase and showed preferential growth along (111)-direction. We obtained the optimal optical and electrical properties of CuI films at the substrate temperature of 120°C . The maximal transmittance is close to 100% and the average transmittance is about 90% in the wavelength region of 410–1500 nm. The lowest resistivity of CuI films is $1.0 \times 10^{-2} \Omega\text{cm}$ with hole concentration and mobility are $3.0 \times 10^{19} \text{ cm}^{-3}$ and $25 \text{ cm}^2 \text{ V}^{-1} \text{ s}^{-1}$, respectively. Increasing substrate temperature degrades the CuI film's semiconductor physical properties. It is believed that the evaporation of a trace amount of iodine from CuI film due to the higher substrate temperature decreasing the concentration of V_{Cu} is the key reason.

Acknowledgements This work was supported by NSFC (11174112, 51472110) and Shandong Provincial Science Foundation for Disguised Youth Scholars (JQ201214). The research programs from Ministry of Education, China, are also acknowledged (NCET-11-1027, 213021A). B. C. thanks the Taishan Scholar Professorship (TSHW20091007) tenured at University of Jinan.

References

[1] H. G. Wang, X. Bai, J. Q. Wei, P. X. Li, Y. Jia, K. L. Wang, and D. H. Wu, *Mater. Lett.* **79**, 106 (2012).

[2] M. De, P. S. Ghosh, and V. M. Rotello, *Adv. Mater.* **20**, 4225 (2008).

[3] G. R. A. Kumara, S. Kaneko, M. Okuya, and K. Tennakone, *Langmuir* **18**, 10493 (2002).

[4] P. Gao, M. Gu, X. Liu, Y. Q. Zheng, and E. W. Shi, *Cryst. Res. Technol.* **47**, 707 (2012).

[5] K. Tennakone, G. R. A. Kumara, I. R. M. Kottegoda, V. P. S. Perera, G. M. L. P. Aponsu, and K. G. U. Wijayanth, *Sol. Energy Mater. Sol. Cells* **55**, 283 (1998).

[6] K. Bädcker, *Phys. Z.* **9**, 431 (1908).

[7] F. L. Schein, H. V. Wenckstern, and M. Grundmann, *Appl. Phys. Lett.* **102**, 092109 (2013).

[8] M. Grundmann, F. L. Schein, M. Lorenz, T. Böntgen, J. Lenzner, and H. V. Wenckstern, *Phys. Status Solidi A* **210**, 1671 (2013).

[9] B. L. Zhu and X. Z. Zhao, *Phys. Status Solidi A* **208**, 91 (2011).

[10] S. Inudo, M. Miyake, and T. Hirato, *Phys. Status Solidi A* **210**, 2395 (2013).

[11] T. Tanaka, K. Kawabata, and M. Hirose, *Thin Solid Films* **281–282**, 179 (1996).

[12] Z. Zheng, A. R. Liu, S. M. Wang, B. J. Huang, K. W. Wong, X. T. Zhang, S. K. Hark, and W. M. Lau, *J. Mater. Chem.* **18**, 852 (2008).

[13] D. Kim, M. Nakayama, O. Kojima, I. Tanaka, H. Ichida, T. Nakanishi, and H. Nishimura, *Phys. Rev. B* **60**, 13879 (1999).

[14] R. P. Vasquez, *Surf. Sci. Spectra* **2**, 149 (1993).

[15] S. Ntais, V. Dracopoulos, and A. Siokou, *J. Mol. Catal. A* **220**, 199 (2004).

[16] J. I. Pankove, *Optical Process in Semiconductors* (Dover Publications, Inc., New York, 1971), p. 3.

[17] P. M. Sirimanne, M. Rusop, T. Shirata, T. Soga, and T. Jimbo, *Chem. Phys. Lett.* **366**, 485 (2002).

[18] B. R. Sankapal, E. Goncalves, A. Ennaoui, and M. C. Lux-Steiner, *Thin Solid Films* **451–452**, 128 (2004).

[19] Y. Y. Zhou, M. K. Lv, G. J. Zhou, S. M. Wang, and S. F. Wang, *Mater. Lett.* **60**, 2184 (2006).

[20] H. L. Kang, R. Liu, K. L. Chen, Y. F. Zheng, and Z. D. Xu, *Electrochim. Acta* **55**, 8121 (2010).

[21] Y. Yang and Q. M. Gao, *Langmuir* **21**, 6866 (2005).

[22] H. Feraoun, H. Aourag, and M. Certier, *Mater. Chem. Phys.* **82**, 597 (2003).

[23] D. G. Chen, Y. J. Wang, Z. Lin, J. K. Huang, X. Z. Chen, D. M. Pan, and F. Huang, *Cryst. Growth Des. Commun.* **10**, 2057 (2010).

[24] P. Gao, M. Gu, X. L. Liu, B. Liu, and S. M. Huang, *Appl. Phys. Lett.* **95**, 221904 (2009).

[25] V. A. Nikitenko and S. G. Stoyukhin, *Opt. Spektrosk.* **54**, 193 (1983).

[26] B. Q. Cao, M. Lorenz, A. Rahm, H. von Wenckstern, C. Czekalla, J. Lenzner, G. Benndorf, and M. Grundmann, *Nanotechnology* **18**, 455707 (2007).

[27] K. Ding, Q. C. Hu, D. G. Chen, Q. H. Zheng, X. G. Xue, and F. Huang, *IEEE Electron Device Lett.* **33**, 1750 (2012).

[28] Y. Kokubun, H. Watanabe, and M. Wada, *Jpn. J. Appl. Phys.* **10**, 864 (1971).